

Aerosol and Air Quality Research

Special Issue on COVID-19 Aerosol

Drivers, Impacts and Mitigation (XIV)

Special Issue:

Challenges in Predicting the Filtration Performance of a Novel Sewn Mask: Scale-up from Filter Holder to Mannequin Measurements

Audrey J. Dang¹, Benjamin M. Kumfer¹, J. Tyler Bertroche^{2‡}, Jane Olson Glidden³, Christopher R. Oxford¹, Udayabhanu Jammalamadaka⁴, Mary Ruppert-Stroescu⁵, Alexander R. Scott⁶, Jason A. Morris⁶, Connie Gan⁶, Jesse Hu⁶, Bradley King⁷, David I.A. Dhanraj¹, Shruti Choudhary¹, Pratim Biswas^{1,8}, Richard L. Axelbaum¹, Kathleen W. Meacham⁹, Brent J. Williams^{1*}

- ¹ Center for Aerosol Science and Engineering, Department of Energy, Environmental and Chemical Engineering, Washington University in St Louis, Saint Louis, MO 63130, USA
- ² Department of Otolaryngology-Head & Neck Surgery, Washington University School of Medicine, St. Louis, MO 63110, USA
- ³ Weavers' Guild of St. Louis, Missouri, USA
- ⁴ Mallinckrodt Institute of Radiology, Washington University in St. Louis School of Medicine, St. Louis, MO 63110, USA
- ⁵ Sam Fox School of Design and Visual Arts, Washington University in St. Louis, Saint Louis, MO 63130, USA
- ⁶ Washington University in St. Louis School of Medicine, St. Louis, MO 63110, USA
- ⁷ Division of Environmental Health & Safety, Washington University in St. Louis, St. Louis, MO 63110, USA
- ⁸ College of Engineering, University of Miami, Coral Gables, FL 33146, USA
- ⁹ Department of Anesthesiology, Washington University in St. Louis School of Medicine, St. Louis, MO 63110, USA

OPEN ACCESS

Received: November 13, 2020 Revised: January 30, 2021 Accepted: February 6, 2021

* Corresponding Author: brentw@wustl.edu

* Present address: Department of Otolaryngology, The Iowa Clinic, West Des Moines, IA 50266, USA

Publisher:

Taiwan Association for Aerosol Research

ISSN: 1680-8584 print **ISSN:** 2071-1409 online

© Copyright: The Author(s). This is an open access article distributed under the terms of the Creative Commons Attribution License (CC BY 4.0), which permits unrestricted use, distribution, and reproduction in any medium, provided the original author and source are cited.

ABSTRACT

Novel designs and materials for filtering face-piece respirators (FFRs) have been disseminated in response to shortages during the COVID-19 pandemic. Since filtration efficiency depends on particle diameter and air face velocity, the relevance of material filtration or prototype fit data depends on test conditions. We investigate whether characterizing a material in a filter holder at a range of face velocities enabled precise prediction of the filtration performance of a novel sewn mask design. While larger particles (> 500 nm) are more relevant for inhalation exposure to respiratory emissions, we compare this mask and a N95 FFR (as a control) with smaller particles more similar to those in the N95 test method. Sewn from sterilization wrap, our mask (sealed to a mannequin head with silicone) filters $85 \pm 1\%$ of 136 nm particles (NaCl, 85 L min^{-1}) and passes quantitative fit tests for 4 of 6 volunteers, representing intermediate protection between a surgical mask and N95 FFR. Filter holder material measurements overpredict the sewn mask's filtration efficiency by 8.2% (95% CI 7.4–9.1%) (136 or 200 nm). While testing flat material in a filter holder enables comparison between materials, filtration performance does not precisely scale-up from filter holder to mannequin tests. Testing full prototypes at relevant conditions is crucial if an improvised design is intended as a substitute for a commercial surgical mask or FFR

Keywords: Respirator, Filtration, Face velocity, COVID-19, Mask



1 INTRODUCTION

During the COVID-19 pandemic, shortages of filtering face-piece respirators (FFRs) and surgical masks have motivated the development and dissemination of improvised mask designs, including sewing patterns, 3D printing files, and recommendations for repurposing alternative materials (Godoy, 2020; Make the Mask, 2020; Strong-Wright, 2020). Surgical masks and FFRs offer different levels of protection against the inhalation of suspended particles. The primary function of the well-fitted FFR is to protect the wearer from inhaling suspended particles which can contain infectious virus. In contrast, the looser fitting surgical mask is primarily intended to capture the user's own emissions, though the user is protected to a level dependent on both material filtration performance and the fit of a particular mask to their face. In the United States, the Food and Drug Administration (FDA) and the National Institute for Occupational Safety and Health (NIOSH) also regulate other attributes of surgical masks and surgical N95 FFRs including fluid resistance (for splatter of bodily fluids) and airflow resistance (pressure drop), which affects breathability and can exacerbate leakage around edges (Office of the Federal Register, 2002; FDA Center for Devices and Radiological Health, 2004; Rengasamy et al., 2014; ASTM International, 2017a; Rengasamy et al., 2017; FDA Office of Product Evaluation and Quality, 2020). During the COVID-19 pandemic, the exposure risk of inhaling suspended particles containing infectious virus has driven increased use of FFRs, especially among healthcare personnel (Cai et al., 2020; Fennelly, 2020; Liu et al., 2020; Miller et al., 2020; Morawska and Milton, 2020; Van Doremalen et al., 2020; Li et al., 2021).

In response to shortages of commercial FFRs, sewn masks fabricated out of sterilization wrap have been used by some healthcare personnel (Godoy, 2020; Ou et al., 2020). Despite crucial differences in test methods, the manufacturer's specification for bacterial filtration efficiency (BFE) of 99.9% may have led to the mistaken perception that sterilization wrap sewn masks might similarly protect the user against much smaller particles, as would a N95 FFR, which had passed the NIOSH particle filtration test (Chen et al., 2020a). However, particle capture mechanisms (inertial impaction, interception, diffusion, electrostatic capture) strongly depend on test conditions, including particle diameter and the face velocity at which air flows through a material. These two variables are essential to interpret filtration test results (Hinds, 1999). In this particular case, the high flowrate and specified particle distribution (75 \pm 20 nm particle diameter number mode, geometric standard deviation < 1.86) of a NIOSH aerosol filtration test should result in decreased filtration efficiency relative to a BFE test (3000 \pm 300 nm particle diameter) (Office of the Federal Register, 2002; Liverman and Alper, 2017; Rengasamy et al., 2017). Indeed, in size-resolved filtration characterization of a dual layer of H600 at a face velocity of 10.5 cm s⁻¹ (reflecting that of a NIOSH test of a typical FFR), Ou et al. (2020) measured a minimum filtration efficiency of 73 \pm 1% for NaCl particles of 100 nm diameter.

Besides material properties, the form of a mask or FFR also impacts mask and FFR filtration efficiency. Particles can infiltrate though leaks between the mask or FFR and the user's face, and consequently, NIOSH requires that users complete annual fit testing which evaluates infiltration of particles through leaks (Rengasamy et al., 2014; Office of the Federal Register, 2019). The form of a mask or FFR also impacts the effective surface area available for filtration, which influences the air face velocity through the material. For the same volumetric flowrate, air will approach a larger surface area with a smaller average face velocity:

$$u = \frac{Q}{A} \tag{1}$$

where u is average face velocity, Q is volumetric flowrate, and A is surface area. Theoretically, when coupled with material characterization at different face velocities, this simple relationship could be used to guide development of more effective improvised mask designs with higher surface area.

The filtration efficiency and breathing resistance of many materials (including household textiles) continues to be characterized at one or more face velocities to inform material selection for face coverings including improvised surgical masks and FFRs (Rengasamy *et al.*, 2010; Davies *et al.*, 2013; Hao *et al.*, 2020; Ou *et al.*, 2020; Pei *et al.*, 2020). We investigate whether material



filtration efficiency measurements at multiple face velocities can enable precise prediction of the performance of a new sewing pattern for a sterilization wrap mask.

2 METHODS

2.1 Materials for Filtration and Pressure Drop Tests

The control FFR was a duckbill-style commercial N95 FFR (3M™ VFlex™ Healthcare Particulate Respirator and Surgical Mask 1804S, 3M, St Paul, MN) (Fig. 1). The test masks followed a novel sewn mask pattern (named the "Glidden"), which is included with detailed step-by-step directions in the Supplementary Material. Key features include multiple sets of ties (one of which acts as a drawstring within a channel under the chin) and pleated folds that facilitate airflow through a larger surface area. Two material combinations were tested with this same Glidden pattern as full masks and as flat material punches in a filter holder. First, a double layer of sterilization wrap (H600, Halyard Health, Alpharetta, GA) was chosen given its off-label use in masks during the COVID-19 pandemic as well as promising tests of fluid resistance (Liu *et al.*, 2020). The second material combination included an intermediate layer of Filti™ Face Mask Material (Filti, Inc., Lenexa, KS, USA, purchased March 30, 2020) between two outer layers of H600. We note that the H600 material can be purchased in multiple configurations (single layer, double layer, double layer of different colors) (Halyard Health, 2020).

Since the masks and FFRs had a complex shape, their surface area was determined by assuming a uniform specific surface area per unit mass (determined by weighing a small square of known area). The filtration surface areas of the N95 FFR and the Glidden design were determined as the product of the specific surface area and the mass of the filtration material (weighed after material not used for filtration (i.e., straps) was removed). For an 85 L min⁻¹ flowrate (which is the flowrate through a single FFR in NIOSH tests of particle filtration efficiency), the average face velocity for the duckbill-style commercial N95 FFR (236 cm²) was 6.0 cm s⁻¹, which is lower than found for FFR designs in other studies (10.6 to 12.9 cm s⁻¹) (Office of the Federal Register, 2002; Bałazy *et al.*, 2006; Rengasamy *et al.*, 2017). The greater surface area of the Glidden mask (415 cm²) yielded an even smaller average velocity of 3.4 cm s⁻¹.

2.2 Filter Holder Measurements of Filtration Efficiency as a Function of Face Velocity

NaCl aerosol was generated with a Collison nebulizer, dried in a diffusion dryer, neutralized (1 mCi Po-210), and then classified using a differential mobility analyzer (DMA) (TSI Inc., model 3080 classifier with model 3081 DMA) with a diameter setpoint of 136, 200, 300, or 466 nm (Fig. 1). The aerosol flowrate through the DMA was controlled by adjusting the house vacuum needle valve to maintain a constant pressure at the exit of the DMA (±0.01 in. H₂O, Dwyer 2001C) regardless of the pressure drop across the filter media. Given the wideness of the DMA transfer function (1.45 L min⁻¹ aerosol flowrate, 5 L min⁻¹ sheath flowrate) as well as multi-charging effects, we describe our measurements as reflecting particle size distributions which result from a given setpoint diameter (instead of a single diameter) (Appendix A1). The classified aerosol was neutralized a second time (1 mCi Po-210), mixed in an annular diluter with HEPA-filtered house air, and then either directed to a bypass line or a 47 mm stainless steel filter holder with a punch of the test filtration material. A condensation particle counter (CPC) (TSI Inc., model 3022A) in high flow mode (1.65 L min⁻¹) measured the particle concentration with house vacuum making up the remainder of the flowrate. Filtration efficiency was calculated as Eq. (2), switching between the filter holder and bypass lines to obtain alternating measurements of CFilter Holder and *C*_{Bypass} respectively:

$$E = 1 - \frac{C_{Filter\ Holder}}{C_{Bypass}\left(\frac{C_{Filter\ Holder,Blank}}{C_{Bypass,Blank}}\right)}$$
(2)

where E is filtration efficiency, and the ratio of C_{Filter Holder,Blank} and C_{Bypass,Blank} corrects the bypass



(a) Aerosol generation, conditioning, and selection

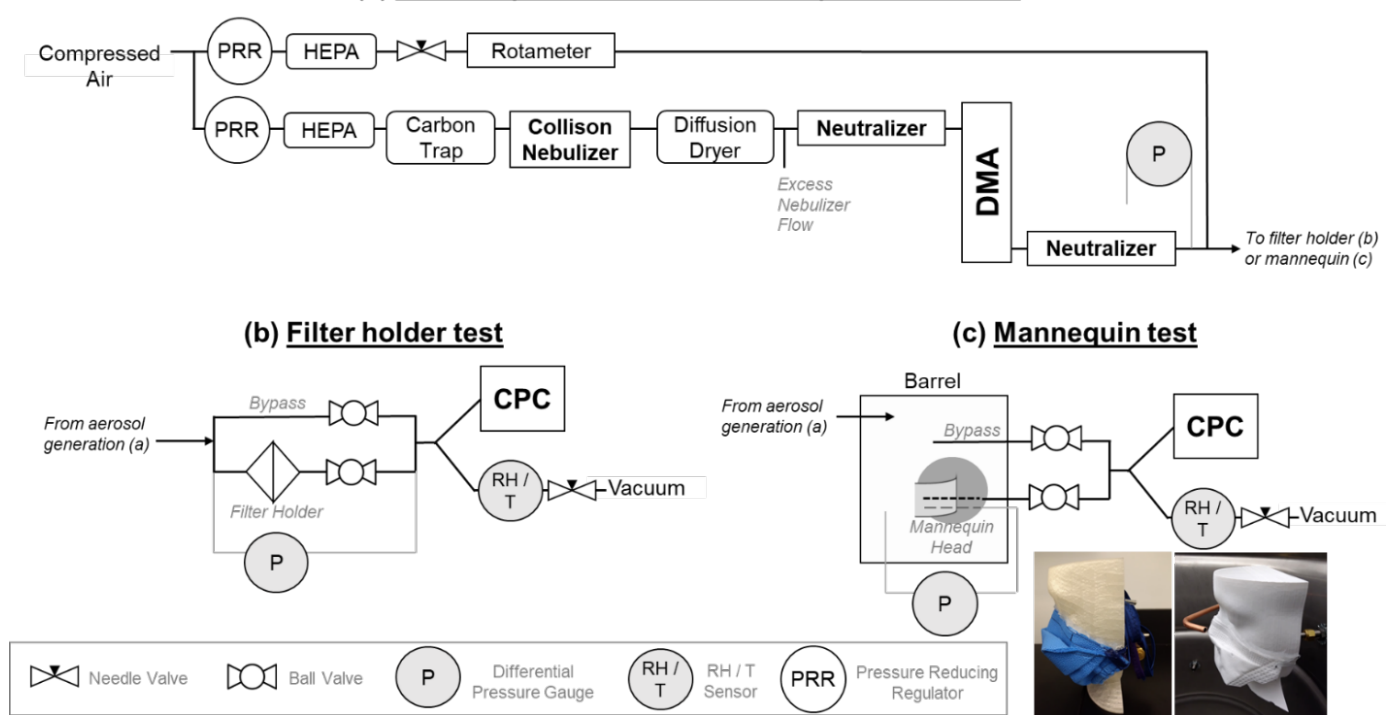


Fig. 1. Flow diagram for (a) generation and conditioning of aerosol for (b) filter holder and (c) mannequin tests. Photographs in (c) are Glidden mask (left) and commercial N95 FFR (right) mounted to 3D-printed mannequin heads for testing.

measurement for particle losses through the empty filter holder (Appendix A2 further describes method of calculations and statistics). For most measurements (including all mannequin measurements and 12 of 16 filter holder measurements), the flow was switched between the bypass and filtered holder lines four times to obtain three unfiltered and two filtered measurements in succession, which were averaged to calculate $C_{Filter\ Holder}$ and C_{Bypass} . We verified that the filtration materials were not themselves shedding particles by capping off the aerosol flow and comparing bypass and filter holder concentrations of HEPA-filtered air (Appendix A2). Temperature and relative humidity were not controlled and ranged from 19 to 22°C and 4 to 32% RH (inversely related to dilution ratio). As described in Appendix A3, we separately fitted the data for each material and particle diameter (for interpolation) using a simplified functional form for filtration efficiency as a function of face velocity (Hinds, 1999).

2.3 Filter Holder Measurements of Pressure Drop as a Function of Face Velocity

The pressure drop across the filtration media in the filter holder was measured (with either Dwyer 2002 or Dwyer 2030C depending on magnitude) over a range of face velocities and was corrected for the pressure drop of the system when the filter holder was empty. As per the relation developed by Davies for a fibrous filter, a first order model with zero intercept was fitted to the pressure drop and face velocity data using least squares regression (Davies, 1973; Hinds, 1999). To increase interpolation precision at face velocities similar to those in the mannequin experiments, only measurements at face velocities < 10 cm s⁻¹ were included in this regression.

2.4 Mannequin Measurements for Filtration Efficiency and Pressure

Similar to Bałazy *et al.* (2006), we sealed the edges of full masks and FFRs onto a mannequin head (3D-printed based on a computed tomography (CT) scan of an adult) with silicone sealant for both pressure and filtration measurements (Bałazy *et al.*, 2006; hv33822, 2020). The mannequin tests used the same aerosol generation and flow control methods as the filter holder tests (Fig. 1). The silicone sealant was applied at least 12 hours prior to testing. Filtered aerosol was



sampled from a 208 L barrel through a 3/8" stainless steel, straight tube, which was installed in the mannequin head with the tube end located right below the mannequin's nostrils. Unfiltered aerosol was sampled through a 3/8" copper bypass tube whose inlet was located near the front of the mannequin head. Temperature and relative humidity (RH) were not controlled and ranged between 20 to 22°C and 4 to 7% RH. For several sewn Glidden masks, a second measurement was performed after adding a bead of silicone sealant over each line of stitching as well as over the ends of any seams.

To measure pressure drop across the mask or FFR, a second tube was installed 1 inch below the first tube in the 3D-printed mannequin head. A differential pressure gauge (Dwyer 2002) measured the pressure difference between this tube and the barrel.

2.5 Quantitative Fit Testing

Quantitative fit testing of the Glidden mask design by volunteers was determined to not be human subjects research by the Washington University in St Louis Institutional Review Board. A TSI Model 8026 Particle Generator augmented ambient particle concentrations with NaCl particles, and fit factors were determined using a PortaCount Respirator Fit Tester Model 8048 and TSI FitPro Ultra software. Three material combinations were tested; all had two outer layers of H600 with an intermediate layer of either Filti (n = 2), a household disposable dusting cloth (n = 2), or a commercial filtration material for heating and air conditioning systems (HVAC) (n = 2). A condensation nuclei counter compared ambient concentrations with those sampled from through a grommet from the interior of the mask. After completing six standard activities, the fit factor was calculated as the ratio of concentrations outside and inside the mask. The overall fit factor was calculated as the product of the number of exercises and the inverse of the sum of the inverses of the individual fit factors (OSHA, 2004). Volunteers included users of both small and regular sizes of commercial FFRs.

3 RESULTS

3.1 Filter Holder Measurements

Particle diameter and face velocity strongly affected the filtration efficiency of flat material punches in a filter holder (Fig. 2). With increasing face velocity up to 60 cm s⁻¹, filtration efficiency decreased for both the commercial N95 FFR material and double layer of H600 sterilization wrap. This trend was also consistent for the three-layer combination (H600-Filti-H600), except at the highest velocity (60 cm s⁻¹) and larger particle diameter distributions (300 nm and 466 nm). With increasing particle diameter, filtration efficiency increased with the exception of the 60 cm s⁻¹ tests for both the commercial N95 FFR material and double layer of H600 sterilization wrap, for which the filtration efficiency of the 466 nm distribution was not significantly different than that measured for the 300 nm distribution. The disruption of trends at the highest face velocity could reflect shifting relative importance of different capture mechanisms. For all materials, pressure drop across the material punches increased linearly with face velocity as would be expected for a fibrous filter material (Davies, 1973; Hinds, 1999).

Our filtration efficiency measurements for a double layer of H600 at 10.6 cm s⁻¹ are 7 to 12% greater than those reported by Ou et~al.~(2020) for the H600 Quick Check product (which is also two layers) at a similar face velocity (10.5 cm s⁻¹). Ou et~al.~(2020) reported a range of $73\pm2\%$ for 100 nm particles to $79\pm1\%$ for 500 nm particles, and our filter holder measurements range from $79.8\pm0.4\%$ for 136 nm particles to $89.2\pm0.2\%$ for 466 nm particles. Our pressure drop measurement (146 Pa, calculated at 10.5 cm s⁻¹ from the linear regression with respect to face velocity) was 8% lower than that measured by Ou et~al.~(2020) (159 Pa) at the same face velocity. If this pressure drop difference reflected a proportional, systematic difference in face velocity measurement, it would result in a bias of only 1% in the filtration efficiency measurement (as per the regression). Multi-charging effects should also not be a large contributor to the discrepancy between our results, since doubly-charged particles of the same mobility (which have double the mass) have comparatively small differences in filtration efficiency. The observed differences in measurements across studies could also be due to normal manufacturing variability, especially since filtration of submicron particles is not a specified property for H600.



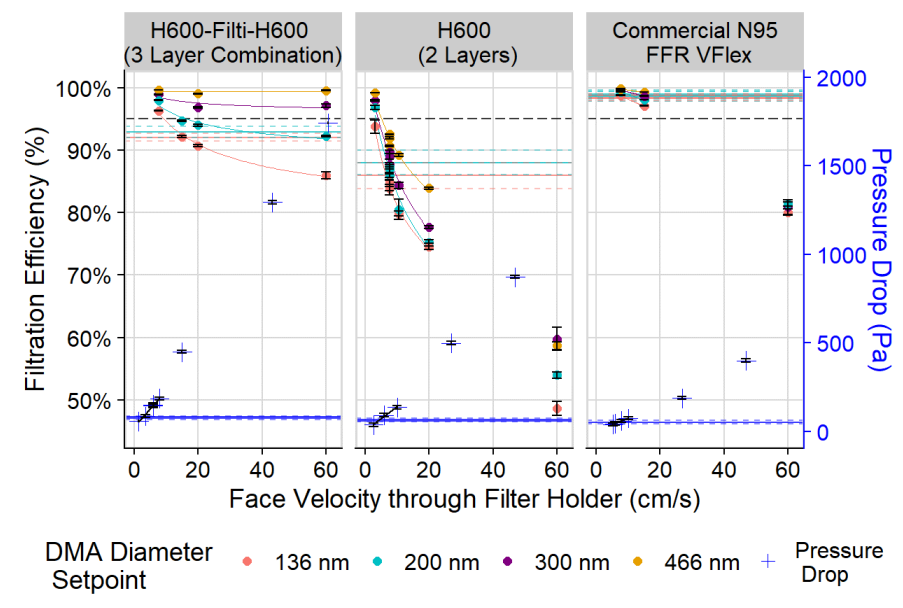


Fig. 2. Filtration efficiency (circle marker) and pressure drop (+ marker) measurements for 47 mm punches in a filter holder are shown as a function of face velocity. Mean mannequin measurements (85 LPM flowrate) for the commercial N95 FFR and the sewn masks (with silicone sealing any stitching or seams) are shown as solid horizontal lines (dashed horizontal lines indicate error intervals).

3.2 Mannequin Measurements

At a flowrate of 85 L min⁻¹, only the commercial N95 FFR filtered more than 95% of the 136 nm or 200 nm distributions in the mannequin tests (Fig. 3, Table A3). When fabricated from a double layer of H600 sterilization wrap, the Glidden sewn mask filtered $85 \pm 1\%$ of particles from the 136 nm distribution, adding a middle layer of Filti material only slightly increased filtration efficiency to $91 \pm 2\%$. When stitching and seams were sealed with a bead of silicone sealant, filtration efficiency increased only 1% and 2% for the sewn Glidden masks in the two-layer (H600-H600) and three-layer (H600-Filti-H600) combinations respectively. Thus, for the H600 material, holes created by stitching and gaps between layers at seams do not play a large role in particle infiltration (at least during initial use).

The mannequin measurements were compared with predictions from the regression models developed for the filter holder measurements and evaluated at the average velocity calculated from the surface area of the FFR (Fig. 3). For the commercial N95 FFR, the mannequin measurement and the prediction from filter holder measurements were not significantly different for the filtration efficiency of the 200 nm distribution and only 0.7% different for the 136 nm distribution. In contrast, the sewn Glidden masks (in both material combinations) performed 8.2% (95% CI 7.4%–9.1%, two-tailed paired t-test) worse than the filter holder measurements predicted at the average face velocity (and using the same material combinations). Infiltration through stitching and seams only accounted for 1.4% of this discrepancy (95% CI 0.7–2.2%).

In a similar comparison for pressure drop, mannequin pressure drops were higher than predicted by filter holder tests for both the commercial N95 FFR or the Glidden sewn mask fabricated from two layers of H600 sterilization wrap. However, the pressure drop of the Glidden sewn mask fabricated from the three layer combination (H600-Filti-H600) was 22% lower than predicted by the filter holder measurements, which could be suggestive of a leak or defect in the masks. All pressure drop mannequin measurements were well below the maximum airflow resistance for N95 FFRs (245 Pa for exhalation, 343 Pa for inhalation) (Office of the Federal Register, 2002). However, in a departure from the NIOSH method, we did not control relative humidity or environmentally condition filtration materials, which would have simulated the effects of moisture from exhaled breath. In addition to affecting filtration for better or worse, moisture could increase pressure drop to the detriment of breathability.



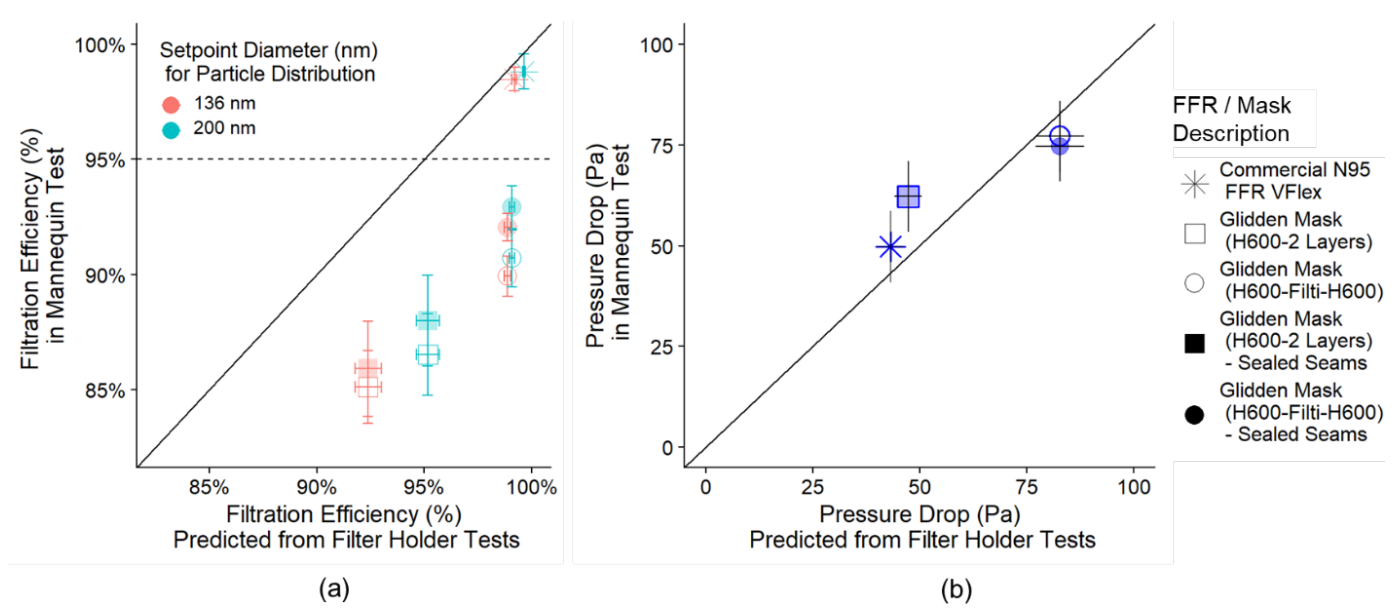


Fig. 3. Comparison of mean (a) filtration efficiency and (b) pressure drop mannequin measurements (85 L min⁻¹) with predictions from the filter holder measurements at the average face velocity calculated from the surface area of the mask.

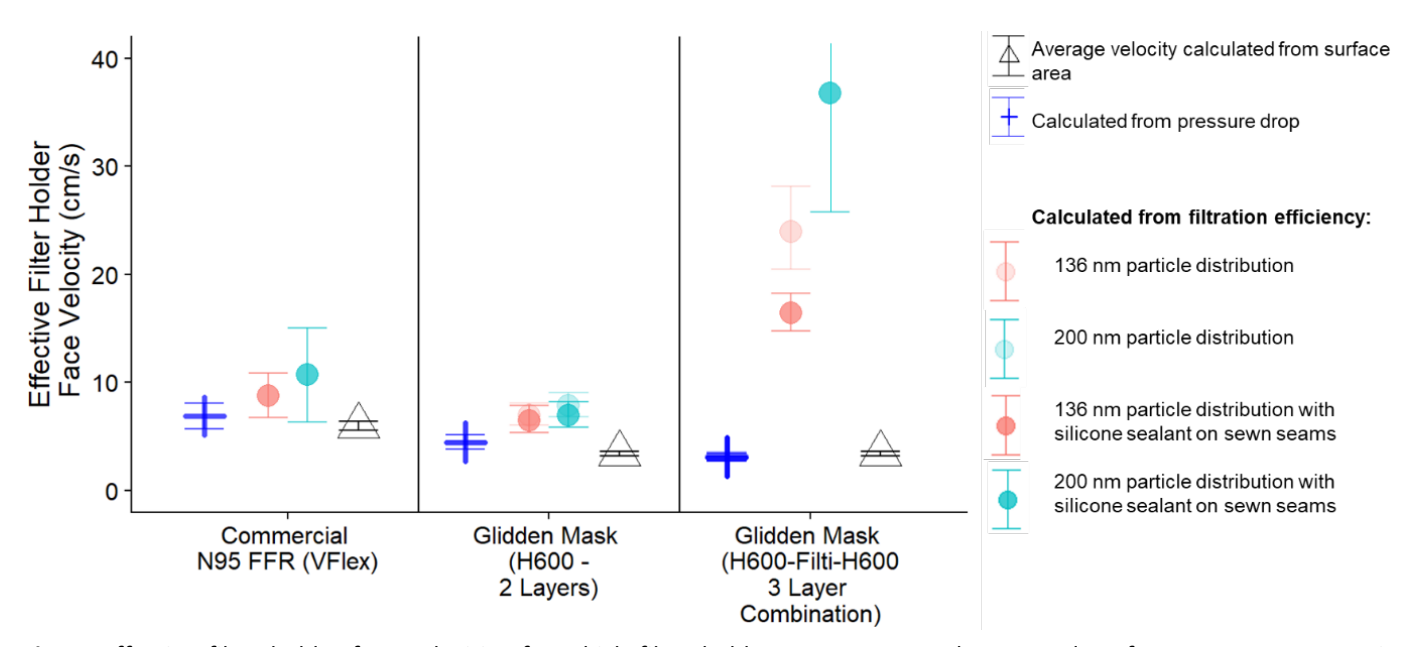


Fig. 4. Effective filter holder face velocities for which filter holder measurements have equal performance to mannequin measurements (filtration and pressure drop) as compared to the average face velocity calculated from the surface area of the full mask (at 85 L min⁻¹).

3.3 Effective Face Velocity Calculations

Since aerosol generation, conditioning, and selection were identical between filter holder and mannequin tests, we hypothesized that variability in face velocity could explain the previously described discrepancies between them. To this end, the regression models were also used to calculate "effective" face velocities at which flat material in the filter holder performed equally to the corresponding mannequin measurements (Fig. 4). There is a distribution of face velocities among the differential areas of the mask or FFR. The measured mannequin pressure drop is the maximum possible across any differential area of the mask or FFR, and thus the effective face velocity for pressure drop represents the maximum face velocity (assuming negligible pressure differences over the external surface of the mask or FFR). An effective face velocity for filtration



efficiency that is greater than the effective face velocity for pressure drop indicates additional particle penetration that cannot be explained by face velocity.

For the N95 FFR, the average face velocity (calculated from surface area) and the effective face velocities (calculated from pressure drop and filtration efficiency) were similar. However, for both Glidden masks, the effective face velocities for filtration efficiency were greater than the face velocities for pressure drop, even when infiltration through stitches and seams was mitigated with a silicone sealant. A leak in masks (whether in the material, stitching/seams, or at the silicone seal between the FFR or mask edge and the mannequin) could cause the observed decreased filtration efficiency, as well as low pressure drop observed for the H600-Filti-H600 Glidden. We note that such a leak would need to be highly consistent across replicate masks, as the measurements are fairly precise (especially with respect to the 8.2% discrepancy between predicted and actual filtration efficiency discussed in the previous section): A range of 2.4% and 2.7% for filtration efficiency of 136 nm and 200 nm particles respectively among replicates of the unsealed H600-H600 Glidden (n = 3), and a range of 0.6% and 0.1% for filtration efficiency of 136 nm and 200 nm particles respectively among replicates of the unsealed H600-Filti-H600 Glidden (n = 2). One difference between filter holder and mannequin measurements is the physical arrangement of the layers. The filter holder tightly clamps the layers of material in contrast to the looser arrangement in the Glidden design (in which layers generally follow the same contour, even at the pleated folds, but are physically joined only at the outer seams).

3.4 Quantitative Fit Testing

4 out of 6 quantitative fit tests with the Glidden mask passed (Table A4). In the two failed cases (scores of 20 and 98 vs. a passing score of 100), the large size of the mask design was noted as problematic. In particular, the long edge across the top of the nose overlapped onto the ears of one volunteer. While material stiffness and plasticity could affect fit, the different filtration properties of the middle layer do not diminish the relevance of a passing score on a quantitative fit test, which reflects the worst-case fit (penalized by particles penetrating both through face seal leaks as well as through the material).

4 DISCUSSION

4.1 What is the Most Relevant Face Velocity for Filter Holder Tests of Particle Filtration?

Since filtration efficiency strongly depends on face velocity and particle diameter, test conditions are crucial for interpreting material filtration tests. However, the most relevant conditions can differ between designs and applications. For the same flowrate, the average face velocity is different among designs of different surface areas (over a factor of two between the Glidden sewn design in this study and previously studied FFRs) (Bałazy *et al.*, 2006; Ou *et al.*, 2020; Strong-Wright, 2020). As an extreme case, some 3D-printed designs have exposed filtration areas as low as 13.5 cm² for which the average face velocity is 105 cm s $^{-1}$ (for the 85 L min $^{-1}$ flowrate of a NIOSH test) (Make the Mask, 2020). Even commercial N95 FFR material filtered only 80.0 \pm 0.5% of 136 nm particles at the highest flowrate (60 cm s $^{-1}$) in our study.

In the absence of a target design, a common face velocity still enables comparison of different materials, but regulatory test methods do not converge upon a single recommended condition (Liverman and Alper, 2017; Rengasamy *et al.*, 2017). For example, the FDA particle filtration efficiency (PFE) test method (ASTM F2299) allows over an order in magnitude in range from 0.5 to 25 cm s⁻¹ (ASTM International, 2017b). This latitude in test method conditions might contribute to previously observed variability in the filtration efficiency of surgical masks, which are categorized into three levels based on this test (Rengasamy *et al.*, 2017; Lam *et al.*, 2020; Schilling *et al.*, 2020). To the same effect, the FDA's bacterial filtration efficiency (BFE) test method (ASTM, 2101) specifies a total flowrate of 28.3 L min⁻¹, but does not specify surface area, essentially permitting a range of face velocities (ASTM International, 2019). Finally, the NIOSH N95 filtration test cannot be applied to a material in isolation from a target design, as the method specifies a total flowrate (85 L min⁻¹) through a single FFR, whose surface area determines the characteristic average face velocity such that this method also yields a range of relevant face velocities (Office of the Federal



Register, 2002). At 85 L min⁻¹, the duckbill-style FFR in this work had a characteristic average face velocity of 6.0 cm s⁻¹ while FFRs in previous studies had characteristic average face velocities of 10.6 to 12.9 cm s⁻¹ (Bałazy *et al.*, 2006).

4.2 The Glidden Design as a Case Study of Scaling up from Filter Holder to Mannequin Tests

Theoretically, a proposed design's surface area could be used to calculate a characteristic average velocity (for the target 85 L min⁻¹ flowrate of the NIOSH test) at which filtration tests could be performed to predict a material's performance in that design. In this work, we tested the validity of this scale-up approach—from material testing in a filter holder to prototype testing with a mannequin. We found that actual performance of a material and design pairing may be estimated, but not necessarily precisely predicted by material filtration tests for a new sewn mask design. Specifically, for a particle distribution with 136 nm setpoint, the Glidden mask in two layers of H600 had a mean filtration efficiency of $85 \pm 1\%$ versus predicted performance of $92 \pm 1\%$ 1%, in the three layer combination (H600-Filti-H600), actual filtration efficiency was 90 \pm 1% versus predicted performance of 98.9 \pm 0.1%. Especially given the high filtration efficiency of the N95 FFR control, the precision of replicate measurements supports that this observation is not an artifact of our methods, which have consistent aerosol generation and measurement methods between the filter holder and mannequin measurements. Rather, as previously discussed in the results section, the scale-up error could derive from leaks in the mask itself, heterogeneity in face velocity, or possibly differences in the spacing between material layers. Regardless of cause, the scale-up error in predictions of mannequin filtration tests from filter holder tests motivates our recommendation to test full prototypes (with the intended material) when a precise, high level of filtration efficiency is required.

The scale-up error from filter holder to mannequin performance (8.2%: 95% CI 7.4–9.1%, two-tailed paired t-test) could be acceptable when designing for use cases in which the user does not expect performance comparable to an N95 FFR (for example, when individuals wear masks to prevent community transmission). Such predictions (which consider the characteristic average face velocity of a specific mask design) are likely superior to design-agnostic predictions (from measurements at much smaller or larger face velocities), though particle penetration around the edges of a poorly fitting mask could substantially decrease actual protection. However, in use cases where an N95 FFR would be preferred if supply was adequate, this scale-up error motivates filtration testing of a full prototype to inform risk analysis weighing an improvised design against competing options for increasing, reusing, and conserving N95 FFR supply.

We also considered whether this example elucidates an alternate heuristic to predict mask performance. Measuring pressure drop with a mannequin or similar set-up may be more experimentally accessible for some designers or users, but this was not a sufficient proxy for determining a relevant filter holder face velocity for filtration (Fig. 4). In addition, since the effective face velocities differed between the two material combinations in the same Glidden design, each pairing of design and material should be separately tested. In fact, using the effective face velocity calculated for the Glidden design in one material to predict the filtration efficiency of the same design in the other material results in a modestly reduced prediction error for the H600-Filti-H600 material combination (6–9% vs. 4–7%), but a much larger prediction error for the double layer of H600 (6–9% vs. –12 to –20%). For this Glidden design, mannequin tests with additional materials (including single layers and possibly a range of flowrates) might help determine under what conditions this consistent prediction error (8.2%: 95% CI 7.4–9.1%, two-tailed paired t-test) might hold.

4.3 Evaluating the Glidden Design: Filtration and Fit

When fabricated with either sterilization wrap material combination studied here, the new mask design (the "Glidden") does not have comparable respiratory protection to a N95 FFR. However, in combination with good filtration efficiency, the superior fit of the Glidden design likely increases protection relative to a surgical mask, as demonstrated in this work by quantitative fit testing by a limited number of volunteers. While fit factors ≥ 98 were achieved among 5 of 6 users of the Glidden mask in this work, Oberg (2008) measured fit factors for surgical masks of only 2.5



to 9.6 among 20 subjects (Oberg and Brosseau, 2008). As currently designed, the Glidden mask is better suited to larger faces, as the two failing fit tests occurred for individuals with small faces. With its simple shape, the pattern could be adjusted for different sized faces by slightly increasing or decreasing the size of the initial material rectangle. Fit testing (equivalent to that required by OSHA for individuals using commercial FFRs) would be similarly important for users of the Glidden mask. In particular, verifying good fit of the drawstring tie in the channel beneath the chin would be key for users accustomed to commercial FFR designs without this feature. Between the two material combinations, the slight improvement in filtration efficiency with an intermediate Filti layer (from $86 \pm 2\%$ to $92 \pm 1\%$) is accompanied by an increase in pressure drop (62–75 Pa). The filter quality factor (Q) describes this compromise:

$$Q = \frac{\ln\left(\frac{1}{1-E}\right)}{\Delta P} \tag{3}$$

where ΔP is the pressure drop. Q is not much improved from 0.033 Pa^{-1} for the double layer combination to 0.035 1/Pa for the triple layer combination (vs. 0.087 Pa^{-1} for the superior commercial N95 FFR) (Hinds, 1999). We emphasize that H600 sterilization wrap (as well as the dusting cloth and HVAC materials included in the quantitative fit testing samples) are not intended for use in face coverings and that other attributes (fluid resistance for healthcare use, biocompatibility, consistency of filtration performance between manufacturing batches) should also be evaluated.

4.4 What are the Relevant Conditions for Mannequin Filtration Tests of Improvised FFR Designs?

As recently emphasized by Chen *et al.* (2020a) and Ou *et al.* (2020), the conditions of filtration test methods are critical for interpreting their results (Rengasamy *et al.*, 2017; Chen *et al.*, 2020a). In addition, when a precise level of filtration is required, the observed discrepancy in scale-up from filter holder to mannequin tests should motivate testing of a specific design and material pairing with particles of a relevant diameter at a relevant flowrate. While not identical to a NIOSH particle filtration test method for N95 FFRs, our mannequin test method was intended to imitate it in the key variables of flowrate and particle diameter. As in the NIOSH test, the mannequin test was performed at 85 L min⁻¹. In addition, we aimed to test particle diameters (136–466 nm) larger than other coronaviruses, but close to those used in a NIOSH N95 particle filtration test (75 \pm 20 nm particle diameter number mode, geometric standard deviation < 1.86) (Office of the Federal Register, 2002; Masters, 2006; Rengasamy *et al.*, 2017).

It is worth noting that particles of these diameters (< 500 nm) are not necessarily those most likely to be involved in community transmission of SARS-CoV-2. While recent characterizations of SARS-CoV-2 describe a distribution of virus diameters between 75 to 105 nm, respiratory particles which could contain this virus are likely much larger and composed primarily of water, proteins, surfactant, and salt (Goldsmith et al., 2004; Marr et al., 2019; Martines et al., 2020). Johnson (2011) describes a characteristic size distribution for particles emitted by speaking and coughing as the sum of three lognormal distributions with different physical origins. Contributing 93% of particle number concentration, the two modes of smallest diameter are at 1600 nm (bronchiolar fluid film burst mode) and 2500 nm (laryngeal mode) (Johnson et al., 2011). Within seconds of emission, respiratory particles in this size range would shrink by at least half (in diameter) at < 90%RH (Marr et al., 2019). Larger respiratory particles might not necessarily contain more infectious virus, as the relationship between particle size and the concentration of infectious virus is currently unknown (Zuo et al., 2013; Yan et al., 2018; Zhou et al., 2018; Santarpia et al., 2020). Particle size would also influence the fate of emitted particles, the probability of exposure in a particular environment, and the probability of deposition among different regions of the respiratory tract, which may also affect infectivity (Hinds, 1999; Chen et al., 2020b).

Given this work's focus on improvised substitutes for N95 FFRs for occupational use among healthcare personnel, our measurements were limited to smaller particle diameters (136–466 nm), as would be the case in a NIOSH particle filtration test for N95 FFRs. If an improvised design was



intended to mitigate a different, non-biological particulate hazard, we would include a 75 nm diameter setpoint, which is the specified number mode for NIOSH filtration testing (Office of the Federal Register, 2002; Rengasamy *et al.*, 2014). In the case of SARS-CoV-2, additional measurements up to 4000 nm may better reflect typical transmission of this respiratory pathogen if particle sizes typical of those produced by human speech or coughing are most likely to result in transmission in a particular situation.

Automating flow control in our experimental set-up would enable efficient characterization at additional diameters. Our motivation in size classification upstream of the filtration material (as opposed to a scanning mobility particle sizing (SMPS) method with a larger range of diameters) was to avoid loading scarce test materials with large amounts of aerosol. Given the lower ambient particle concentrations in a hospital environment relative to other occupational environments, we aimed to characterize the FFRs and masks with no to little particle loading, though the NIOSH method measures changes with increased particle loading (Li et al., 2012; Rengasamy et al., 2017).

As for flowrate, our study replicated the 85 L min⁻¹ flowrate used in NIOSH test methods, thus achieving relevant face velocities for each mask and FFR design (Liverman and Alper, 2017; Rengasamy et al., 2017). The presence of the mannequin may have altered how the air flowed through the mask as compared to the NIOSH method. We note that 85 L min⁻¹ is a reasonable estimate of peak inspiratory flowrate among healthcare personnel. To investigate variability among different occupations, Caretti et al. (2004) developed empirical relationships between oxygen consumption, minute ventilation rate, and peak inspiratory flowrate. For patient care (which Caretti et al. categorize as light to moderate standing activity), these relationships yield minute ventilation rates of 24.6 L min⁻¹ for female individuals and 28.1 L min⁻¹ for male individuals, which correspond to estimated peak inspiratory flowrates (83 and 94 L min⁻¹) which are quite similar to that of the NIOSH test method (85 L min⁻¹). Even higher peak inspiratory flowrates (93–116 L min⁻¹) would be expected when healthcare personnel engage in moderate to heavy activity while standing (defined as lifting > 50 lbs, which would be the case while lifting patients, during which close physical distance would also increase exposure risk) (Caretti et al., 2004). While an individual is only momentarily breathing at the peak inspiratory flowrate, exposure is weighted by instantaneous flowrate, such that some have recommended further testing of respiratory protection PPE at higher flowrates (Holmér et al., 2007). While we do not consider it reasonable to subject improvised designs to a higher flowrate than specified in the NIOSH test method, we also do not find justification to lower the test flowrate below 85 L min⁻¹ solely based on intended use among healthcare personnel.

In our mannequin tests, edges were sealed with silicone sealant, such that we could evaluate the penetration of particles through the filter media itself. In practice, both routes of particle infiltration (through and around the filter media) contribute to exposure and should be evaluated. Test methods which do not control face velocity/flowrate or particle diameter (ex. qualitative fit testing with sucrose or Bitrex, quantitative fit testing with the TSI Portacount) provide faster, lower cost, and more accessible comparison for rapid evaluation during prototyping, especially when optimizing designs for fit (van der Sande *et al.*, 2008; TSI Incorporated, 2013; Byrne *et al.*, 2020; Mueller *et al.*, 2020; Woolverton *et al.*, 2020). However, if the intended use case is substitution of a regulated respiratory device in a crisis shortage, more rigorous filtration testing at relevant test conditions is necessary to understand how filtration performance compares with that of the substituted commercial FFR.

While we have focused on face velocity and particle diameter in this work, another key test condition is particle charge neutralization for consistent testing of electrostatic capture (which is a significant filtration mechanism for many commercial N95 materials as well as H600) (Ou *et al.*, 2020). In addition, prior to NIOSH particle filtration testing, N95 FFRs are environmentally conditioned to simulate moisture uptake from exhaled breath, (Office of the Federal Register, 2002). Implementing environmental conditioning would be particularly important if wearers of preliminary prototypes noted changes in air resistance after prolonged use.

5 CONCLUSION

Filtration testing of materials at relevant particle diameters and face velocities are valuable for



evaluating materials used in any face covering, including improvised masks or N95 FFRs for healthcare personnel. Our work demonstrates that even when detailed material filtration testing is available, filtration testing of the improvised design itself (fabricated with the intended material) is critical if a specific threshold of filtration performance must be verified, as is the case when developing improvised substitutes for N95 FFRs. While valuable for rapid evaluating the fit of a new design, qualitative and quantitative fit testing is not equivalent to high quality filtration testing of prototypes at relevant particle diameters and flowrates. Developing capacity for high quality filtration testing should be prioritized if improvised designs are required to compensate for insufficient supply, and the lack of such data should strongly factor into risk analyses of stopgap measures during crisis shortages.

ACKNOWLEDGEMENTS

AJD acknowledges support from a National Science Foundation Graduate Research Fellowship (DGE-1745038). BJW acknowledges support from NSF CAREER (CBET award number 1554061) and the Alfred P. Sloan Foundation (Chemistry of Indoor Environments) for laboratory materials utilized in this study. Any opinions, findings, and conclusions or recommendations expressed in this material are those of the authors and do not necessarily reflect the views of the National Science Foundation. KWM received salary support from an International Anesthesiology Research Society Mentored Research Award.

The authors thank the PPE Safety Consortium at Washington University in St. Louis. We also thank the WUSTL McKelvey School of Engineering, notably Megan Flake, for providing assistance and ensuring necessary safety precautions during COVID-19 laboratory restrictions.

SUPPLEMENTARY MATERIAL

Supplementary data associated with this article can be found in the online version at https://doi.org/10.4209/aaqr.200629

REFERENCES

- ASTM International (2017a). Standard Test Method for Resistance of Medical Face Masks to Penetration by Synthetic Blood (Horizontal Projection of Fixed Volume at a Known Velocity). F1862 / F1862M.
- ASTM International (2017b). Standard Test Method for Determining the Initial Efficiency of Materials Used in Medical Face Masks to Penetration by Particulates Using Latex Spheres. ASTM F2299 / F2299M 03.
- ASTM International (2019). Standard Test Method for Evaluating the Bacterial Filtration Efficiency (BFE) of Medical Face Mask Materials, Using a Biological Aerosol of Staphylococcus aureus. ASTM F2101.
- Bałazy, A., Toivola, M., Reponen, T., Podgorski, A., Podgorski, P., Zimmer, A., Grinshpun, S.A. (2006). Manikin-based performance evaluation of N95 filtering-facepiece respirators challenged with nanoparticles. Ann. Occup. Hyg. 50, 259–269. https://doi.org/10.1093/annhyg/mei058
- Byrne, J.D., Wentworth, A.J., Chai, P.R., Huang, H.W., Babaee, S., Li, C., Becker, S.L., Tov, C., Min, S., Traverso, G. (2020). Injection Molded Autoclavable, Scalable, Conformable (iMASC) system for aerosol-based protection: A prospective single-arm feasibility study. BMJ Open 10, e039120.
- Cai, J., Sun, W., Huang, J., Gamber, M., Wu, J., He, G. (2020). Indirect virus transmission in cluster of COVID-19 cases, Wenzhou, China, 2020. Emerging Infect. Dis. 26, 1343–1345. https://doi.org/10.3201/EID2606.200412
- Caretti, D.M., Gardner, P.D., Coyne, K.M. (2004). Workplace breathing rates: Defining anticipated values and ranges for respirator certification testing, Oak Ridge Institute for Science and Education, Oak Ridge.
- Chen, V., Long, K., Woodburn, E.V. (2020a) When weighing universal precautions, filtration



- efficiency is not universal. J. Hosp. Infect. 105, 412–413. https://doi.org/10.1016/j.jhin.2020.0 4.032
- Chen, W., Zhang, N., Wei, J., Yen, H.L., Li, Y. (2020b). Short-range airborne route dominates exposure of respiratory infection during close contact. Build. Environ. 176, 1–16. https://doi.org/10.1016/j.buildenv.2020.106859
- Davies, A., Thompson, K.A., Giri, K., Kafatos, G., Walker, J., Bennett, A. (2013). Testing the efficacy of homemade masks: Would they protect in an influenza pandemic? Disaster Med. Public Health Prep. 7, 413–418. https://doi.org/10.1017/dmp.2013.43
- Davies, C. (1973) Air filtration, Academic Press, London.
- Embodi3D (2020). Face stl, https://www.embodi3d.com/files/file/33684-face-stl/ (accessed 14 April 2020).
- FDA Center for Devices and Radiological Health (2004). Surgical Masks Premarket Notification [510(k)] Submissions. FDA-2003-D-0305.
- FDA Office of Product Evaluation and Quality (2020). Enforcement Policy for Face Masks and Respirators During the Coronavirus Disease (COVID-19) Public Health Emergency (Revised): Guidance for Industry and Food and Drug Administration Staff.
- Fennelly, K.P. (2020). Particle sizes of infectious aerosols: Implications for infection control. Lancet Respir. Med. 8, 914–924. https://doi.org/10.1016/S2213-2600(20)30323-4
- Godoy, G. (2020). Facial protection for healthcare workers during pandemics: A scoping review. BMJ Glob. Health 5, e002553. https://doi.org/10.1136/bmjgh-2020-002553
- Goldsmith, C.S., Tatti, K.M., Ksiazek, T.G., Rollin, P.E., Comer, J.A., Lee, W.W., Rota, P.A., Bankamp, B., Bellini, W.J., Zaki, S.R. (2004). Ultrastructural characterization of SARS coronavirus. Emerging Infect. Dis. 10, 320–326. https://doi.org/10.3201/eid1002.030913
- Halyard Health (2020). Sterilization Wrap. https://www.halyardhealth.com/solutions/surgical-solutions/sterilization-solutions/sterilization-wrap.aspx (accessed 12 November 2020).
- Hao, W., Parasch, A., Williams, S., Li, J., Ma, H., Burken, J., Wang, Y. (2020). Filtration performances of non-medical materials as candidates for manufacturing facemasks and respirators. Int. J. Hyg. Environ. Health 229, 113582. https://doi.org/10.1016/j.ijheh.2020.113582
- Hinds, W.C. (1999). Aerosol Technology, 2nd ed. Wiley, Hoboken.
- Holmér, I., Kuklane, K., Gao, C. (2007). Minute volumes and inspiratory flow rates during exhaustive treadmill walking using respirators. Ann. Occup. Hyg. 51, 327–335. https://doi.org/10.1093/annhyg/mem004
- Johnson, G.R., Morawska, L., Ristovski, Z.D., Hargreaves, M., Mengersen, K., Chao, C.Y.H., Wan, M.P., Li, Y., Xie, X., Katoshevski, D., Corbett, S. (2011). Modality of human expired aerosol size distributions. J. Aerosol Sci. 42, 839–851. https://doi.org/10.1016/j.jaerosci.2011.07.009
- Lam, S.C., Suen, L.K.P., Cheung, T.C.C. (2020). Global risk to the community and clinical setting: Flocking of fake masks and protective gears during the COVID-19 pandemic. Am. J. Infect. Control 48, 964–965. https://doi.org/10.1016/j.ajic.2020.05.008
- Li, L., Zuo, Z., Japuntich, D.A., Pui, D.Y.H. (2012). Evaluation of filter media for particle number, surface area and mass penetrations. Ann. Occup. Hyg. 56, 581–594. https://doi.org/10.1093/annhyg/mes034
- Li, Y., Qian, H., Hang, J., Chen, X., Cheng, P., Ling, H., Wang, S., Liang, P., Li, J., Xiao, S., Wei, J., Liu, L., Cowling, B.J., Kang, M. (2021). Probable airborne transmission of SARS-CoV-2 in a poorly ventilated restaurant. Build. Environ. 196, 107788. https://doi.org/10.1016/j.buildenv.2021.107788
- Liu, Y., Ning, Z., Chen, Y., Guo, M., Liu, Y., Gali, N.K., Sun, L., Duan, Y., Cai, J., Westerdahl, D., Liu, X., Xu, K., Ho, K.F., Kan, H., Fu, Q., Lan, K. (2020). Aerodynamic analysis of SARS-CoV-2 in two Wuhan hospitals. Nature 582, 557–560. https://doi.org/10.1038/s41586-020-2271-3
- Liverman, C.T., Alper, J. (2017). Integration of FDA and NIOSH Processes Used to Evaluate Respiratory Protective Devices for Health Care Workers: Proceedings of a Workshop. National Academies of Sciences, Engineering and Mathematics, Washington. https://doi.org/10.17226/23679
- Marr, L.C., Tang, J.W., Van Mullekom, J., Lakdawala, S.S. (2019). Mechanistic insights into the effect of humidity on airborne influenza virus survival, transmission and incidence. J. R. Soc. Interface 16, 20180298. https://doi.org/10.1098/rsif.2018.0298
- Martines, R.B., Ritter, J.M., Matkovic, E., Gary, J., Bollweg, B.C., Bullock, H., Goldsmith, C.S., Silva-



- Flannery, L., Seixas, J.N., Reagan-Steiner, S., Uyeki, T., Denison, A., Bhatnagar, J., Shieh, W.J., Zaki, S.R. (2020). Pathology and pathogenesis of SARS-CoV-2 associated with fatal coronavirus disease, United States. Emerging Infect. Dis. 26, 2005–2015. https://doi.org/10.3201/eid2609. 202095
- Masters, P.S. (2006). The molecular biology of coronaviruses. Adv. Virus Res. 65, 193–292. https://doi.org/10.1016/S0065-3527(06)66005-3
- Miller, S.L., Nazaroff, W.W., Jimenez, J.L., Boerstra, A., Buonanno, G., Dancer, S.J., Kurnitski, J., Marr, L.C., Morawska, L., Noakes, C. (2021). Transmission of SARS-CoV-2 by inhalation of respiratory aerosol in the Skagit Valley Chorale superspreading event. Indoor Air 31, 314–323. https://doi.org/10.1111/ina.12751
- Montana Mask Filter Frame with Flange. https://github.com/blackbear/make-the-masks/tree/master/cad (accessed 7 July 2020).
- Morawska, L., Milton, D.K. (2020). It is time to address airborne transmission of coronavirus disease 2019 (COVID-19). Clin. Infect. Dis. 71, 2311–2313. https://doi.org/10.1093/cid/ciaa939
- Mueller, A.V., Eden, M.J., Oakes, J.M., Bellini, C., Fernandez, L.A. (2020). Quantitative method for comparative assessment of particle removal efficiency of fabric masks as alternatives to standard surgical masks for PPE. Matter 3, 950–962. https://doi.org/10.1016/j.matt.2020.07.006
- Oberg, T., Brosseau, L.M. (2008) Surgical mask filter and fit performance. Am. J. Infect. Control 36, 276–282. https://doi.org/10.1016/j.ajic.2007.07.008
- Office of the Federal Register (2002). Air-Purifying Particulate Respirators. Code of Federal Regulations, Part 84, Title 42.
- Office of the Federal Register (2019). Respiratory protection. Code of Federal Regulations, Part 29, Title 1910.134.
- OSHA (2004). 1910.134 App A Fit Testing Procedures (Mandatory). 69 FR 46993.
- Ou, Q., Pei, C., Kim S.C., Abell, E., Pui, D.Y.H. (2020). Evaluation of decontamination methods for commercial and alternative respirator and mask materials view from filtration aspect. J. Aerosol Sci. 150, 105609. https://doi.org/10.1016/j.jaerosci.2020.105609
- Pei, C., Ou, Q., Kim, S.C., Chen, S.C., Pui, D.Y.H. (2020) Alternative face masks made of common materials for general public: Fractional filtration efficiency and breathability perspective. Aerosol Air Qual. Res. 20, 1–11. https://doi.org/10.4209/aaqr.2020.07.0423
- Rengasamy, S., Eimer, B., Shaffer, R.E. (2010). Simple respiratory protection-evaluation of the filtration performance of cloth masks and common fabric materials against 20-1000 nm size particles. Ann. Occup. Hyg. 54, 789–798. https://doi.org/10.1093/annhyg/meq044
- Rengasamy, S., Eimer, B.C., Szalajda, J. (2014). A quantitative assessment of the total inward leakage of nacl aerosol representing submicron-size bioaerosol through N95 filtering facepiece respirators and surgical masks. J. Occup. Environ. Hyg. 11, 388–396. https://doi.org/10.1080/15459624.2013.866715
- Rengasamy, S., Shaffer, R., Williams, B., Smit, S. (2017). A comparison of facemask and respirator filtration test methods. J. Occup. Environ. Hyg. 14, 92–103. https://doi.org/10.1080/15459624. 2016.1225157
- Santarpia, J.L., Herrera, V.L., Rivera, D.N., Ratnesar-Shumate, S., Reid, S.P., Denton, P.W., Martens, J.W.S., Fang, Y., Conoan, N., Callahan, M.V., Lawler, J.V., Brett-Major, D.M., Lowe, J.J. (2020). The infectious nature of patient-generated SARS-CoV-2 aerosol. medRxiv 2020.07.13.20041632. https://doi.org/10.1101/2020.07.13.20041632
- Schilling, K., Gentner, D., Wilen, L., Medina, A., Buehler, C., Perez-Lorenzo, L.J., Godri Pollitt, K.J., Bergemann, R., Bernardo, N., Peccia, J., Wilczynski, V., Lattanza, L. (2020). An accessible method for screening aerosol filtration identifies poor-performing commercial masks and respirators. SSRN J. https://doi.org/10.2139/ssrn.3592485
- Strong-Wright, J. (2020). A brief review of materials and designs for homemade masks to protect against COVID-19. Preprints 2020, 2020060132. https://doi.org/10.20944/preprints202006.01 32.v1
- TSI Incorporated (2013). Portacount Pro [®] Model 8030 Respirator Fit Tester Theory of Operation. RFT-002.
- van der Sande, M., Teunis, P., Sabel, R. (2008). Professional and home-made face masks reduce exposure to respiratory infections among the general population. PLoS One 3, e2618. https://doi.org/10.1371/journal.pone.0002618



- Van Doremalen, N., Bushmaker, T., Morris, D.H., Holbrook, M.G., Gamble, A., Williamson, B.N., Tamin, A., Harcourt, J.L., Thornburg, N.J., Gerber, S.I., Lloyd-Smith, J.O., de Wit, E., Munster, V.J. (2020). Aerosol and surface stability of SARS-CoV-2 as compared with SARS-CoV-1. N. Engl J. Med. 382, 1564–1567. https://doi.org/10.1056/NEJMc2004973
- Woolverton, C.J., Ferdig, R.E., Snyder, A., Reed, J., Dodson, T., Thomas, S. (2020). Repurposing surgical wrap textiles for use as protective masks during pandemic response. Appl. Biosaf. 25, 127–129. https://doi.org/10.1177/1535676020925958
- Yan, J., Grantham, M., Pantelic, J., Mesquita, P.J.B. de, Albert, B., Liu, F., Ehrman, S., Milton, D.K., Consortium, E. (2018). Infectious virus in exhaled breath of symptomatic seasonal influenza cases from a college community. PNAS 115, 1081–1086. https://doi.org/10.1073/pnas.171656 1115
- Zhou, J., Wei, J., Choy, K.T., Sia, S.F., Rowlands, D.K., Yu, D., Wu, C.Y., Lindsley, W.G., Cowling, B.J., McDevitt, J., Peiris, M., Li, Y., Yen, H.L. (2018). Defining the sizes of airborne particles that mediate influenza transmission in ferrets. PNAS 115, E2386–E2392. https://doi.org/10.1073/pnas.1716771115
- Zuo, Z, Kuehn, T.H., Verma, H., Kumar, S., Goyal, S.M., Appert, J., Raynor, P.C., Ge, S., Pui, D.Y.H. (2013). Association of airborne virus infectivity and survivability with its carrier particle size. Aerosol Sci. Technol. 47, 373–382. https://doi.org/10.1080/02786826.2012.754841